RSC Advances

This is an *Accepted Manuscript*, which has been through the Royal Society of Chemistry peer review process and has been accepted for publication.

Accepted Manuscripts are published online shortly after acceptance, before technical editing, formatting and proof reading. Using this free service, authors can make their results available to the community, in citable form, before we publish the edited article. This *Accepted Manuscript* will be replaced by the edited, formatted and paginated article as soon as this is available.

You can find more information about *Accepted Manuscripts* in the Information for Authors.

Please note that technical editing may introduce minor changes to the text and/or graphics, which may alter content. The journal's standard Terms & Conditions and the Ethical guidelines still apply. In no event shall the Royal Society of Chemistry be held responsible for any errors or omissions in this *Accepted Manuscript* or any consequences arising from the use of any information it contains.

ROYAL SOCIETY OF CHEMISTRY

www.rsc.org/advances

Please do not adjust margins

Journal Name

ARTICLE

One/two-Photon-Sensitive Photoacid Generators Based on Benzene Oligomer-containing D-π-A-type Aryl Dialkylsulfonium Salts

Received 00th January 20xx,
Accepted 00th January 20xx

DOI: 10.1039/x0xx00000x

www.rsc.org/

Ming Jin,*[a] Xingyu Wu,[a] Jianchao Xie,[a] Jean Pierre Malval*[b] and Decheng Wan[a]

Novel sulfonium-based D-π-A photoacid generators (PAGs) with a benzene oligomer (from one to four) as a π-conjugated system that are highly photosensitive in the near-ultraviolet region (365 nm) were prepared. The maximum absorption and molar extinction coefficients of the PAGs redshifted and enhanced with the increasing length of the conjugated systems. The quantum yields of PAGs were high (three of them were over 0.6) and improved by adjusting the number of the phenyl rings. The quantum chemical calculation results proved that the molecular configuration and nature of the frontier orbitals are crucial factors to affect PAG performance. Photopolymerization kinetic results demonstrated that these sulfonium-based PAGs were highly efficient cationic photoinitiators, and the i-line sensitivities were evaluated based on the photolithographic performance of the PAG-containing SU-8 resins. In addition, the two-photon absorption cross sections (δ_{700nm} > 400 GM) matched the requirements needed in the 3D fabrication of polymer microstructures.

Introduction

The use of sulfonium salt photoacid generators (PAGs)[1, 2] for the production of H^+ upon irradiation is a subject that has attracted increasing interest because they can be used to activate a wide variety of reactions,[3-5] including the ring opening of epoxides and oxetanes,[4-12] as well as cleavage reactions,[13-16] which are commonly used in numerous applications in photoresists,[17] micro-electronics,[18] photosensitized resins,[19] and photodynamic therapy.[20] To date, most commercial sulfonium salt PAGs need ultraviolet light (λ < 300 nm) to achieve cleavage, thereby limiting their applications.[17, 21, 22] Thus, how to redshift their absorption peaks is a topic of much research, and a good method for solving this problem is to enlarge the conjugated systems in the PAGs to prolong the absorption to near-UV and visible spectral regions.[23-27] However, fabricating efficient PAGs with near-UV and visible light irradiation has undergone slow progress since the extension of electronic conjugation of the chromophore often deceases the quantum yield of acid generation (Φ_H^+), as suggested by Belfield et al.[25] Saeva et al. developed a series of anthracenyl and naphthacenyl sulfonium salt derivatives,[28] and these PAGs showed λ_{max} values up to 388–488 nm. However, the values of PAG quantum yields (Φ_H^+) were relatively low (Φ_H^+ < 0.28). In 2002, Perry et al. reported the fabrication of a sulfonium-based PAG whose λ_{max} was 390 nm and exhibited a high quantum yield for acid generation (Φ_H^+ = 0.5).[24] Recently, we also reported a series of D-π-A-type PAGs with substituted-stilbene as π-conjugated systems, in which a methyl(benzyl)sulfonium salt PAG that was monosubstituted in the meta-position of conjugated system redshifted its λ_{max} up to 400 nm while kept excellent performance in photoacid generation (Φ_H^+ = 0.5).[26, 29-31]

Meanwhile, PAGs with enlarged π-conjugated systems always exhibit two-photon absorption (2PA) properties,[24-26, 30, 32-34] in which a molecule simultaneously absorbs two photons at longer wavelengths in the same quantum event.[35] 2PA has two advantages over linear absorbance.[36] First, 2PA probability depends quadratically on the excitation intensity, and the photochemistry can be confined to a small volume of a cube in the excitation wavelength by tightly focusing a laser beam. Second, the linear absorption of aromatic rings in the materials can be neglected when a near-infrared laser is used. Perry et al. reported a sulfonium-based PAG that exhibited large 2PA cross section (δ) (δ_{max} = 690 GM) by introducing bis[(diarylamino)styryl] benzene derivative.[24] The sulfonium salt groups symmetrically bonded on one of the benzene rings of the arylamino moieties. This D-π-D system provided the most effective two-photon sensitivity reported yet (the value of $\Phi_H^+ \cdot \delta$ reaches 345 GM at 710 nm). Our D-π-A-type PAG also exhibited effective two-photon sensitivity ($\Phi_H^+ \cdot \delta$ = 324 GM at 800 nm).[31] Obviously, the structure of the π-conjugated system in sulfonium salts is crucial, and how to systemically adjust is an interesting issue in the field.[37]

[a] School of Materials &Engineering, Tongji University, 4800 CaoAn Road, Shanghai, China. Fax: 86 21 69580143; Tel: 86 21 69580143; E-mail: mingjin@tongji.edu.cn
[b] Institut de Science des Matériaux de Mulhouse, UMR CNRS 7361, Université de Haute-Alsace, 15 rue Jean Starcky, 68057 Mulhouse, France. E-mail: jean-pierre.malval@uha.fr

Electronic Supplementary Information (ESI) available: Details of the organic synthesis and characterization, Photodecomposition, photoacid generation, TGA curves, photopolymerization, photolithography and Two-photon absorption. See DOI: 10.1039/x0xx00000x

RSC Advances Accepted Manuscript

Please do not adjust margins

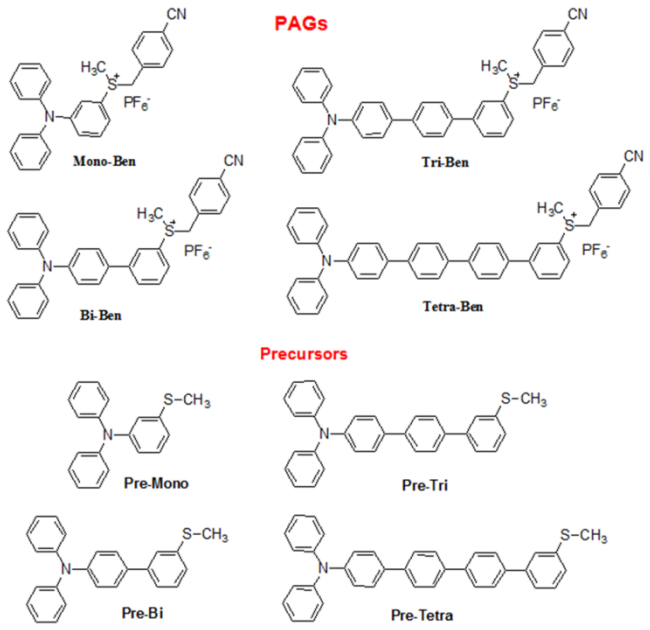

Scheme 1. Molecular structures of PAGs and their corresponding precursors.

Therefore, based on the results of Perry et al.[24] and our own experiences,[26, 30, 31] four sulfonium salts were designed (PAGs in Scheme 1). Diphenylamino group was still selected as the electron donor because it has strong electron-donating ability and its protonated product is a strong acid (Ph_3N^+H, $pK_a = -5$).[38] Methyl(4-cyanobenzyl) sulfonium salt substituted on the meta-position of π-conjugated systems was used because it can effectively adjust the absorption wavelength and influence the photolysis efficiency in sulfonium salt PAGs.[26, 30, 31] The main difference of the PAGs is the π-conjugated systems, in which Mono-Ben, Bi-Ben, Tri-Ben, and Tetra-Ben were introduced to construct one/two-photon active H^+ production systems. The variation in π-conjugated length was expected to adjust and optimize the photochemical and photophysical properties of PAGs, which were then used as promising photoinitiators for the cationic polymerization and lithography with a typical photopolymer SU-8 resin under irradiation in either one- or two-photon mode.

Experimental

Materials. The PAGs and precursors investigated here are presented in Scheme 1 and used with the best purity available. All chemicals for synthesis were purchased from Sinopharm Chemical Reagent Co., Ltd., TCI, Alfa Aesar, or J&K Chemical, and they were used without further purification unless otherwise specified. Cyclohexane Oxide (CHO), N-vinylcarbazole (NVK), methyl diethanolamine (MDEA), tri(ethylene glycol) divinyl ether (DVE), (3,4-epoxycyclohexane)methyl 3,4-epoxycyclohexylcarboxylate (EPOX) and trimethylolpropane triacrylate (TMPTA) were purchased from Sigma-Aldrich or Alfa Aesar from the highest purity available and used as received without further purification. All the solvents employed for photophysical measurements were Fluka spectroscopic grade.

General instrumentations. UV-vis spectra were recorded on a Mapada UV-6300 spectrophotometer. ^{1}H NMR and ^{13}C NMR measurements were recorded by Bruker 400M NMR spectrometer and chemical shifts were reported in parts per million (ppm) downfield from the Me_4Si resonance which was used as the internal standard when recording ^{1}H NMR spectra. Mass spectra were recorded on a Micromass GCTTM and a Micromass LCTTM. The steady-state fluorescence experiments were performed on a Varian Cary Eclipses fluorescence spectrometer. Photolithography pictures were collected with a bright-field microscopy (Nikon-Ti, Co. Ltd. Japan). The GPC were tested by WATERS TD-SEC.

Photodecomposition and photoacid generations. The photodecomposition processes in solution of acetonitrile were studied by UV-vis spectra under irradiation of 365 nm at different intensities. Quantum yields for acid generation were measured under irradiation at 365 nm using a LED spotlight (Uvata, Shanghai). All irradiated PAGs dissolved in acetonitrile were previously N_2-degassed. The progress of the photoreaction was monitored via UV–vis absorption spectra. The absorbance at the excitation wavelength ($A_{365\ nm}$) was greater than 2.5 to assume a total absorption of the incident photons. The dose rates were kept sufficiently small so that the changes of $A_{365\ nm}$ were lower than 10 %. The Rhodamine B (RhB) was used as a sensor of photoacid generation.[39] The acid generation in acetonitrile was also evaluated from a calibration curve of RhB which was gradually protonated by addition of p-toluenesulfonic acid. Then, photoacid quantum yields were calculated according to the equation.[40]

Computational procedure. Molecular orbital calculations were carried out with the Gaussian 09 package with the density functional theory at the B3LYP/6-31 G(d) level and the geometries were frequency checked (ESI).

Photopolymerization. The photopolymerization was monitored *in situ* by Fourier transform real-time infrared spectroscopy (FT-RTIR) with a Thermo-Nicolet iS-5 instrument IR-spectrometer. A drop of the photocurable formulation is deposited on a ATR window or KBr pellet then spread out with a calibrated bar. The aerated film which exhibits an average thickness of 40 µm is irradiated at 365 nm using a 365 nm spotlight (Uvata, Shanghai). The evolution of the epoxy group content of CHO, EPOX, the double bond content of TMPTA and the double bond content of DVE were continuously followed by real time FTIR spectroscopy at about 790 cm^{-1}, 790 cm^{-1}, 1630 cm^{-1} and 1620 cm^{-1}, respectively[41-46]. The conversion of the functional groups is determined by measuring the peak area of these bands at each time of the equation [C (%) = (A_0 - A_t)/A_0 x 100] where C is the degree of conversion of functional groups at t time, A_0 the initial peak area before irradiation and A_t the peak area of the functional groups at t time.

Photolithography. The one-photon lithography was performed using SU-8 photoresist (SU-8 2005 from NanJing Baisiyou Tech Co., Ltd) which was specifically purchased without any photoinitiator. The photoresist was mixed with PAG (1 wt %). The formulation was spin-coated on glass substrates leading to

RSC Advances Accepted Manuscript

This journal is © The Royal Society of Chemistry 20xx

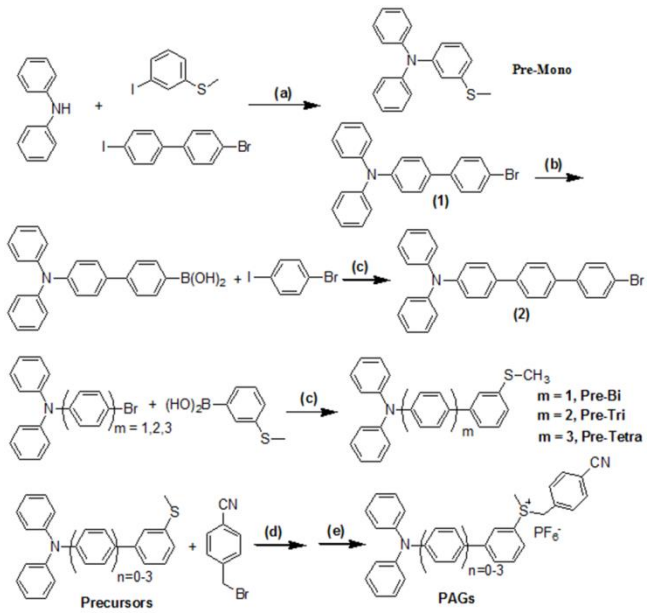

Scheme 2. Synthetic route of the precursors and PAGs. a) Cu, K_2CO_3, N_2, 200 °C, 48 h, 1,2-dichlorobenzene; b) n-BuLi, triisopropyl borate, THF, −78 °C; c) K_2CO_3, $Pd(P(Ph)_3)_4$, toluene, EtOH, water, 100 °C; d) $AgCF_3SO_3$, Cs_2CO_3, CH_2Cl_2, RT; e) KPF_6, water, acetone.

regular films whose thickness (~ 1 μm) was measured by profilometry. The irradiation intensity at 365 nm was fixed at 16 mW cm^{-2}. The procedure for photolithography can be described as follows: *(i)* Spin-coating (3000 rpm) on a Si substrate which was previously pre-treated upon immersion into a piranha solution during 3h at 80 °C. *(ii)* Edge bead removal and 3 min soft baking at 90 °C. *(iii)* Photopatterning upon irradiation at 365 nm during needed time. *(iv)* 3 min post-baking at 90 °C leading to the appearance of the μ-structure *(v)* Final development by rinsing with isopropanol or with cyclohexanone.

Two-photon absorption and microfabrication. Two-photon absorption cross-sections of PAG in DMF were tested by nonlinear absorption method.[47] The same formulation and process was used to prepare the films for two-photon lithography.[48-50] A mode-locked Ti: Sapphire laser system (Tsunami, Spectra-Physics) with a central wavelength of 780 nm, a pulse width of 100 fs, and a repetition rate of 82 MHz was employed to fabricate the 3D microstructures. The laser beam was tightly focused into the photoresist by an oil-immersion objective lens with a high numerical aperture (100 ×, NA = 1.45, Olympus). The photoresist on the glass substrate was moved through the focus spot by a 3D piezostage (P-563.3CL, Physik Instrumente) controlled by a computer. The final structure was obtained after washing to remove the unpolymerized photoresist. The 3D microstructures were characterized by a field-emission scanning electron microscope (SEM, S-4300, Hitachi, Japan).

Synthesis of Precursors and PAGs. The synthetic routes of Precursors and PAGs were shown in Scheme 2. PAGs were prepared by Savea's methods.[28, 37, 51, 52] All detailed synthetic procedures, characterization were shown in the supporting information (Figs S1-12 ESI).

Results and discussion

Photophysical properties of the PAGs. All PAGs showed good solubility in the solvents used in this study (Table S1, ESI). The absorption spectra of all PAGs in acetonitrile were shown in Fig. 1 and the corresponding spectroscopic data are listed in Table 1. All PAGs exhibited intensive absorption in the range of 250–400 nm. The maximum absorption peaks redshifted from 292 nm for Mono-Ben to 351 nm for Tetra-Ben. The redshift of λ_{abs} was only 7 nm when the number of benzene rings increased from 2 to 4. This should be attributed to the single bond between the phenyl rings that influenced the co-planarity of the conjugated systems, as confirmed by the fully optimized structures of PAGs calculated at the DFT level (Fig. S13, Table S2,ESI) . Moreover, the maximum molar extinction coefficients (ε_{max}) increased from 13400 M^{-1} cm^{-1} to 26700 M^{-1} cm^{-1} (Table 1) due to the extensive π-conjugate length in these D-π-A systems.

The molar extinction coefficients of all PAGs were smaller than those of their corresponding precursors, as shown in Table 1 and Fig. S14 (ESI). The absorption spectra of Mono-Ben (Black curve in Fig. 1) had an additional feature on the low energy side of the spectra that was assigned to π-σ* transition.[38] Fig. 2 showed the frontier orbitals of the precursor (Pre-Tri as sample) and all PAGs calculated at the DFT level, which implied obvious electronic delocalization.[53] In the precursor, a very slight charge transfer from the amino group to the conjugated moieties (HOMO-LUMO) was observed in the entire compound structure (π-π* type). However, for the PAGs, the HOMO-LUMO orbitals showed a charge transfer from the amino groups to the sulfonium, and the π-σ* type transition overlapped with the π-π* transition.[52] As such, the former could not be clearly observed, except for that in Mono-Ben because the chemical reactions involving the change in the precursors to the sulfonium salts alter the nature of electron transitions. The calculated energies of the electronic transitions of PAGs and their corresponding oscillator strengths were summarized in Table S3 (ESI), which suggested the longest wavelength

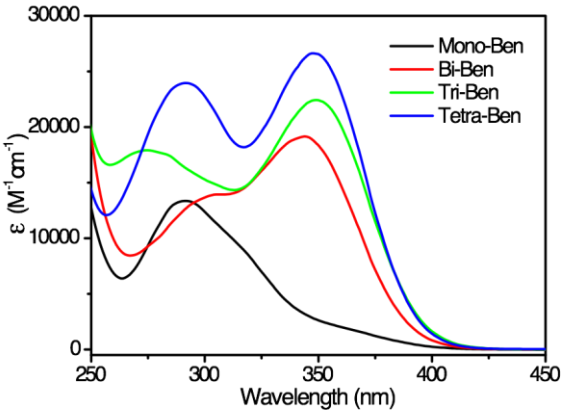

Fig. 1. UV-vis spectra of PAGs in acetonitrile.

RSC Advances Accepted Manuscript

Table 1 Summary of optical data and parameters of PAGs and precursors (Pre) in acetonitrile

Compounds	λ_{abs} (nm)	ε_{max} (M^{-1} cm^{-1})	Δε (Pre-PAG)	Φ_f	Φ_H^{+a}	δ_{max} (GM) [b]
Mono-Ben	292	13400	5400	-	0.60	184
Bi-Ben	344	19300	3200	-	0.69	230
Tri-Ben	349	23500	4700	-	0.73	474
Tetra-Ben	351	26700	11800	-	0.42	393
Pre-Mono	298	17800	-	0.10	-	
Pre-Bi	327	22500	-	0.57	-	
Pre-Tri	345	28200	-	0.78	-	
Pre-Tetra	347	38500	-	0.70	-	

[a] Irradiated at 365 nm, and the uncertainty is in the order of 10%. [b]Nonlinear absorption measurement, the uncertainty of δ is in the order of 20% in DMF.

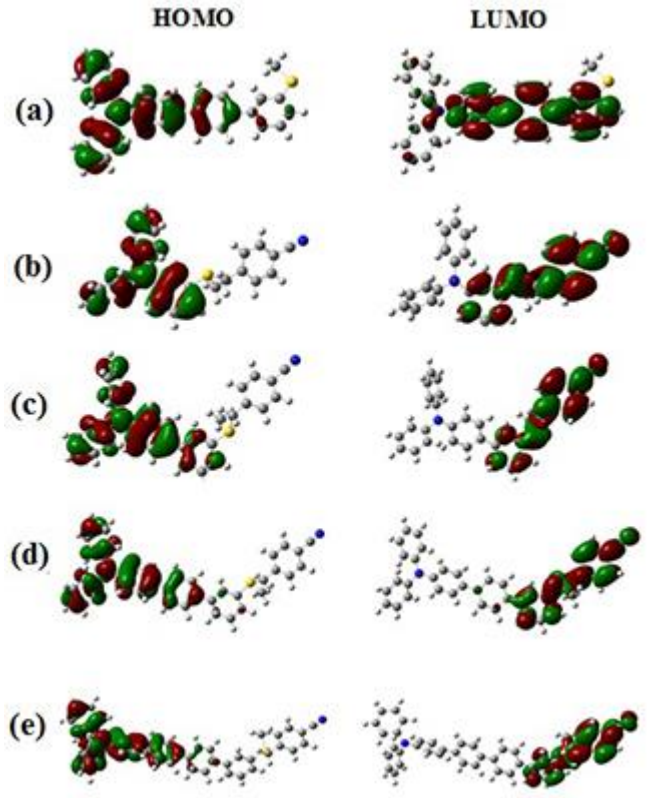

Fig. 2. Highest occupied molecular orbital (HOMO) and lowest unoccupied molecular orbital (LUMO) of Pre-Tri (a) and four PAGs (b-e) at the DFT B3LYP/6-31 G(d) level.

electronic transition was strongly allowed ($f > 1$). The π-σ* type transition had smaller molar extinction coefficients (ε) than the π-π* type transition. Thus, ε of PAGs was lower compared with that of their precursors, and the π-σ* type transition character implied that the PAGs had good Φ_H^+ performance.[37]

The photoexcitation process of PAGs was then examined. The dark stability was first checked, and the results showed that all of the remaining rates were higher than 99%. Detailed photolysis at an excitation wavelength of 365 nm was performed and analyzed via UV-vis spectroscopy, as shown in Fig. 3 and Fig. S15 (see ESI). The decreased absorption of the strongest transition for all PAGs suggested the successful photolysis of the sulfonium salts (Proposed mechanism was shown in Scheme S1, ESI). The quantum yields for photoacid generation (Φ_H^+) reported in Table 1 were measured in acetonitrile using rhodamine B as an acid indicator via the method reported by Scaiano et al.[39] (see Figs. S16 and S17 in ESI). The efficiency of acid generation was strongly dependent on the length of the conjugated systems. For instance, Φ_H^+ of Mono-Ben was 0.60, which was higher than that reported by Perry's group.[38] This improvement was achieved simply by changing 4-cyanobenzyl into benzyl groups in the sulfonium salts. For Bi-Ben and Tri-Ben, the values were higher and reached 0.69 and 0.73, respectively. The high sensitivity of PAGs could be attributed to the better leaving propensity of the 4-cyanobenzyl group and meta-positioned substitution of sulfonium.[31, 54] The chemical shift in ^{1}H NMR spectra could provide some information about the electromagnetic shielding in the molecule. After comparision, it was found that the signals for the protons around the sulfonium salt were downfield shift with the increasing number of benzene rings from 1 to 3 (see Fig. S18 in ESI). This was consistent with the results of the corresponding Φ_H^+ values of PAGs. The futher extention of π-conjugation[25] as for Tetra-Ben PAG decreased

RSC Advances Accepted Manuscript

This journal is © The Royal Society of Chemistry 20xx

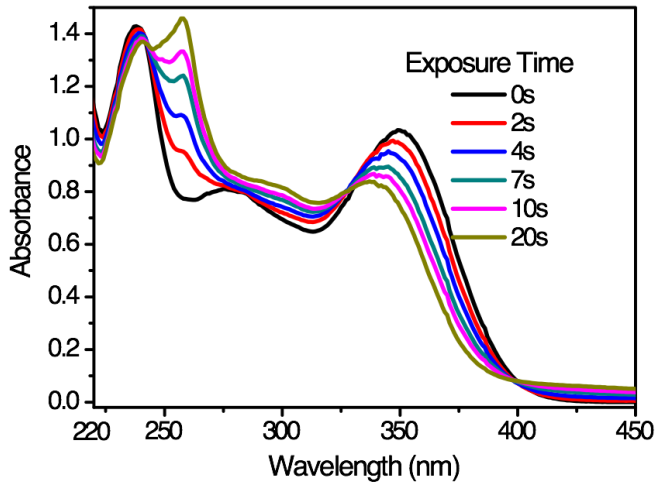

Fig. 3. Evolution of the absorption spectra of Tri-Ben upon irradiation at 365 nm (0.5 mW cm^{-2}). (Solvent: acetonitrile)

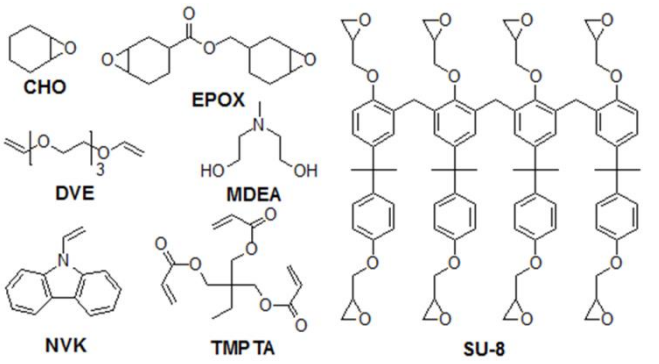

Scheme 3. Chemical structures of the monomers and additives.

Φ_H^+ value to 0.42, however, it was still a high value compared with those reported for PAGs with long wavelength absorption.[28] Therefore, the use of benzene oligomers as conjugated systems was beneficial in improving the performance of PAGs. The appropriate length of the benzene oligomer is crucial in obtaining good Φ_H^+ values, and Tri-Ben generally showed the best performance.

Photopolymerization. The effective efficiency for H^+ photogeneration of PAGs was evaluated by multiplying Φ_H^+ with ε_λ. The latter parameter represents the photon-induced ability to generate excited species upon excitation at a special wavelength, whereas the first factor indicates the quantum yield to produce H^+ from the excited species. In Table 2, the corresponding values are reported for $\Phi_H^+.\varepsilon_{365\ nm}$. The result showed that the efficiency of Mono-Ben was lowest because of its small molar extinction coefficient at 365 nm (1750 $M^{-1}\,cm^{-1}$), and Tri-Ben had the best efficiency. To corroborate these preliminary trends of the photoinitiating efficiencies of PAG, cationic photopolymerizations were performed on CHO (see Scheme 3).[23, 38, 55-57] Fig. 4 shows the FT-RTIR kinetic curves during irradiation of the formulations containing PAGs (1 wt%) at 365 nm. The corresponding values for the maximum polymerization rate ($R_p/[M_0]$) were listed in Table 2. The photoinitiation efficiencies

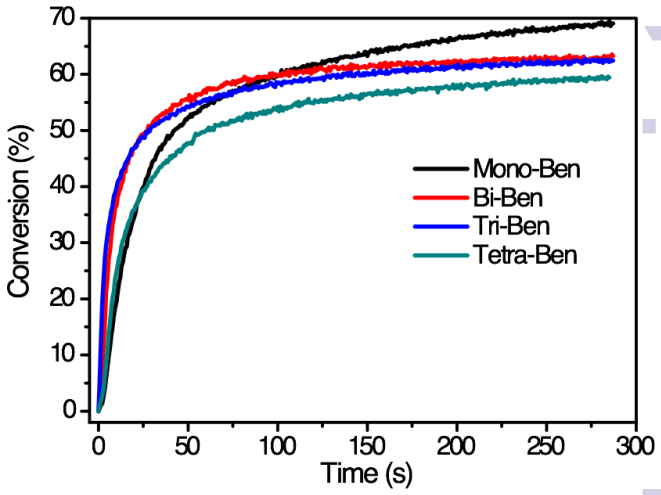

Fig. 4. Conversion vs. time curves for the cationic photopolymerization of CH containing PAGs (1 wt%). λ_{exc}: 365 nm, Irradiance: 5 mW cm^{-2}.

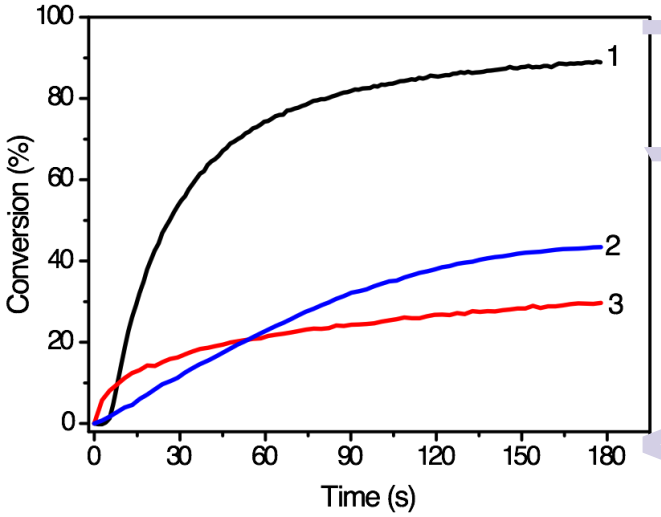

Fig. 5. Photopolymerization profiles of DVE (1 wt% Tri-Ben, curve 1), TMPTA (Tri-Ben/MEDA, 1%/2%, w/w, curve 2), and EPOX (Tri-Ben/NVK, 1%/3%, w/w, curve 3). λ_{exc}: 365 nm, irradiance: 15 mW cm^{-2}.

were clearly correlated with $\Phi_H^+.\varepsilon_{365nm}$. For instance, Tri-Ben underwent rapid photopolymerization with an epoxide conversion rate of 30% after 5 s of irradiation. Bi-Ben exhibited a comparable kinetic curve but with a lower $R_p/[M_0]$ than Tri-Ben, and it had a final conversion of about 60% after 300 s of irradiation. Finally, Mono-Ben, whose $\Phi_H^+.\varepsilon_{365nm}$ was more than one order of magnitude lower than those of the other PAGs, showed a slightly slow dynamic of conversion with an initial induction period of ~3 s and a final conversion of 70% because it has the smallest molecular weight at the same amount of doping at 1 wt%. In addition, the GPC curves of the prepared polymers were tested, and the results are shown in Table 2. The four PAGs showed similar initiating abilities. M_n was around 3000, and PDI was around 1.5. In addition, these PAGs could also be used as photoinitiators for different monomers (see Scheme 3), including EPOX, vinyl ether (DVE), and acrylates (TMPTA), via cationic or free radical polymerizations. The four PAGs showed good photoinitiating

RSC Advances Accepted Manuscript

Table 2 Effective acid generation efficiencies upon excitation at 365 nm, molecular weights of polymers obtained upon various PAGs as initiators, and energy threshold during the lithography of SU-8.

PAGs	$\Phi_H^+ \bullet \varepsilon_{365nm}$ [a] /M^{-1} cm^{-1}	$R_p/[M_0]$ [b] /s^{-1}	M_n [b]	M_w/M_n [b]	Conversion [b] /%	E_{th} [c] /mJ cm^{-2}
Mono-Ben	1050	1.61	3200	1.57	69.1	28
Bi-Ben	8480	4.74	3100	1.48	63.2	10
Tri-Ben	12900	6.28	3100	1.49	62.4	10
Tetra-Ben	8370	2.60	2850	1.48	59.4	20

[a] Tested in acetonitrile; [b] Obtained via the polymerization of cyclohexane oxide (CHO); [c] Energy threshold of the i-line photolithography using a 21-step sensitivity guide

abilities for DVE (Fig S19), and comparable abilities for EPOX and TMPTA as shown in Fig. 5 for Tri-Ben. All PAGs exhibited considerable conversion rates.

One- and two-photon lithographic performance. Traditional near-UV lithography is still being continuously developed by improving exposure tools and fabricating photoresist materials with improved performance both in terms of photosensitivity and resolution.[18] Accordingly, chemically amplified (CA) i-line photoresists[58-60] are probably a better choice than conventional novolac–DNQ-based photoresists. However, reports on chemically amplified i-line resists are relatively scarce because most PAGs used in CA resists usually absorb light below 300 nm.[17] In this work, the prepared PAGs could efficiently generate HPF_6 when exposed to 365 nm UV light, which inspired us to prepared a novel type of CA i-line photoresists with these PAGs and SU-8 resins.

Resist films (1 wt% PAGs in SU-8 2005) on silicon wafers were formed via the same procedures as described in the experimental section. The thermal stabilities of PAGs were tested via TGA, and the decomposition temperature exceeded 150 °C(as shown in Fig. S20, ESI). The films were then exposed to light on a Stouffer 21 step sensitivity guide without a mas The intensity of 365 nm light was 16 mW/cm^2, and the exposure time was 10 s. The prepared photolithograph pictures are shown in Fig. S21 (ESI). Using Mono-Ben as an example, the formed steps of the SU-8 photoresists were directly detected after standard exposure and development. The patterns were clearly engraved on the surface of the wafer. In the fifth step, the wafer was very clear. In the sixth step, some residual polymers were still observed. Finally, in the seventh step, no residual polymer was observed. These results confirmed that the energy at the sixth step was weak, and the energy at the fifth step should be sufficient to crosslink the SU-8 resin. The energy threshold (E_{th}) was calculated as 28 mJ/cm^2. For Bi-Ben, Tri-Ben, and Tetra-Ben, the corresponding steps were 8, 8, and 6, and the E_{th} values were 10, 10, and 20 mJ/cm^2, respectively (see Table 2). The B Ben and Tri-Ben systems could undergo lithography at low photon doses.

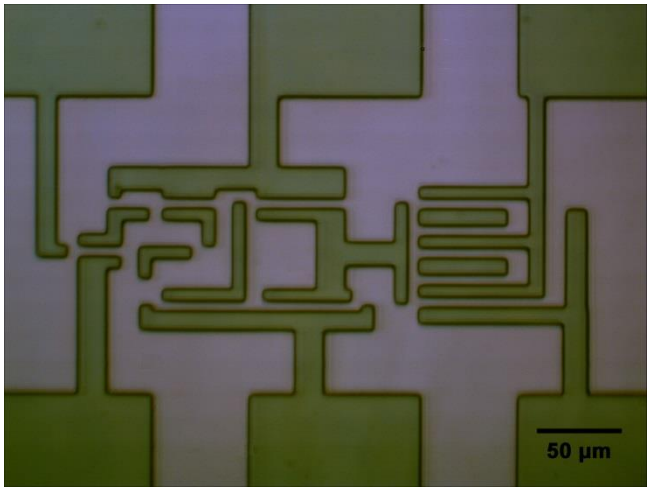

Fig. 6. Example of lines written via one-photon lithography using SU-8 resin containing Tri-Ben (1 wt%). (λ_{exc}: 365 nm, irradiation dose: 25 mJ cm^{-2}).

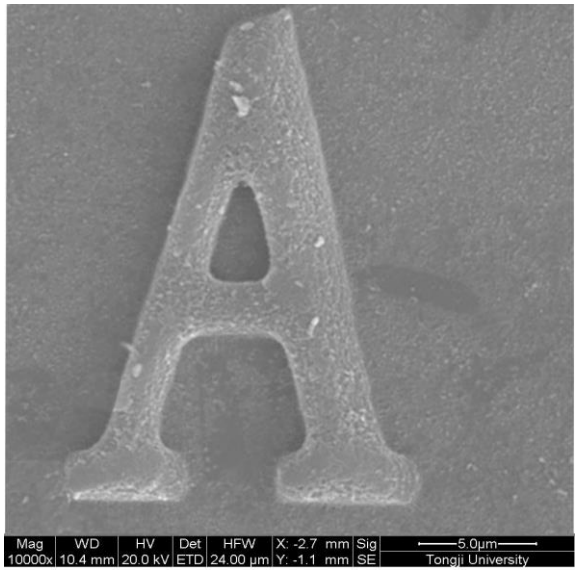

Fig. 7. SEM image of a microstructure fabricated upon excitation at 780 nm (< P > = 15 mW, v = 5 µm s^{-1}). Formulation: SU-8 resin with Tri-Ben (1 wt%).

RSC Advances Accepted Manuscript

This journal is © The Royal Society of Chemistry 20xx

To further demonstrate the potential applications of these π-conjugated PAGs for i-line resists, several 2D microstructures were prepared using the SU-8 resin, which is a highly viscous epoxy-based negative photoresist and widely employed in microelectronics. The resin was mixed with Tri-Ben (1 wt%) and spin-coated on Si substrates to form micrometer-thick films. Fig. 6 shows the optical transmission microscopy image of a photo-patterned microcircuit, which was developed after 20 mJ/cm^2 irradiation (twofold higher than E_{th}). The regular pattern exhibits minimum line width of about 3.0 μm, which is in good accordance with the optical spatial dimension of the photomask.

In addition, the four PAGs showed two-photon absorption cross sections ranging from 180 GM to 470 GM at 700 nm tested by nonlinear absorption in DMF (as shown in Table 1 and Fig. S22, ESI). Tri-Ben also exhibited the highest value, which was thus selected for two-photon lithography processing the same film preparation and development. Fig. 7 shows the scanning electron microscopy (SEM) images of an arbitrary 2D microstructure. By the laser-scanning lithography (LSL) at 780 nm, photoresists SU-8 can be effectively two-photon polymerized and only occurs near the focus of a laser beam. In the part out of the laser focus, the polymerization reaction did not take place and the photoresists are easily washed out by development. Thus, a microobject "A" can be successfully fabricated with a spatial resolution of approximately 1 μm. Hence, using two distinct lithography methods, we successfully demonstrated the potential of these new and highly reactive PAGs for relevant applications in microelectronics technology.

Conclusions

The photoreactivity of a new series of sulfonium-based PAGs with benzene oligomer as π-conjugated systems was evaluated. It was showed that the length of the conjugated system had a significant effect on the linear absorption bands. The extended and twisted conjugated systems extended the absorption peaks to near-UV range, increased the molar extinction coefficients and led to the increase in the quantum yield for acid generation (Φ_H^+ = 0.73 for a triphenyl-containing PAG, Tri-Ben). From a practical perspective, we also demonstrated the photoinitiating performances of these PAGs, in which the conversion of the photopolymerization was correlated very well with the reactivities of these photoinitiators. Finally, the one- and two-photon lithography of Tri-Ben PAG with SU-8 resin exhibited potential and promising applications in i-line chemically amplified photoresists and microfabrication technologies.

Acknowledgements

This work was supported by the National Natural Science Foundation of China (20902069, 51173134). Fundamental Research Funds for the Central Universities and the Open Measuring Fund for Large Instrument and Equipment, Tongji University. Supports from the Agence Nationale de la Recherche "Projet Blanc: 2PAGmicrofab (ANR-BLAN-0815-03)" are also gratefully acknowledged.

References

1. E. Reichmanis and F. Thompson Larry, in *Polymers in Microlithography*, American Chemical Society, 1989, vol. 412, pp. 1-24.
2. E. Reichmanis, F. M. Houlihan, O. Nalamasu and T. X. Neenan, in *Polymers for Microelectronics*, American Chemical Society, 1993, vol. 537, pp. 2-24.
3. J. P. Fouassier, D. Burr and J. V. Crivello, *Journal of Macromolecular Science-Pure and Applied Chemistry*, 1994, **A31**, 677-701.
4. J. V. Crivello and M. Sangermano, *Journal of Polymer Science Part a-Polymer Chemistry*, 2001, **39**, 343-356.
5. J. V. Crivello, *Journal of Polymer Science Part a-Polymer Chemistry*, 1999, **37**, 4241-4254.
6. J. V. Crivello, *Journal of Polymer Science Part a-Polymer Chemistry*, 2007, **45**, 3759-3769.
7. J. V. Crivello, *Journal of Macromolecular Science Part a-Pure and Applied Chemistry*, 2009, **46**, 474-483.
8. J. V. Crivello and U. Bulut, *Journal of Polymer Science Part a-Polymer Chemistry*, 2005, **43**, 5217-5231.
9. J. V. Crivello and S. S. Liu, *Chemistry of Materials*, 1998, **10**, 3724-3731.
10. J. V. Crivello and R. Narayan, *Macromolecules*, 1996, **29**, 439-445.
11. J. V. Crivello and R. A. Ortiz, *Journal of Polymer Science Part a-Polymer Chemistry*, 2002, **40**, 2298-2309.
12. J. V. Crivello, S. Rajaraman, W. A. Mowers and S. S. Liu, *Macromolecular Symposia*, 2000, **157**, 109-119.
13. Y. H. Chen, T. Yamamura and K. Igarashi, *Journal of Polymer Science Part a-Polymer Chemistry*, 2000, **38**, 90-100.
14. J. D. Cho and J. W. Hong, *European Polymer Journal*, 2005, **41**, 367-374.
15. D. Dossow, Q. Q. Zhu, G. Hizal, Y. Yagci and W. Schnabel, *Polymer*, 1996, **37**, 2821-2826.
16. Y. Y. Durmaz, N. Moszner and Y. Yagci, *Macromolecules*, 2008, **41**, 6714-6718.
17. M. Shirai and M. Tsunooka, *Progress in Polymer Science*, 1996, **21**, 1-45.
18. M. Shirai and H. Okamura, *Progress in Organic Coatings*, 2009, **64**, 175-181.
19. C. L. Chochos, E. Ismailova, C. Brochon, N. Leclerc, R. Tiron, C. Sourd, P. Bandelier, J. Foucher, H. Ridaoui, A. Dirani, O. Soppera, D. Perret, C. Brault, C. A. Serra and G. Hadziioannou, *Advanced Materials*, 2009, **21**, 1121-1125.
20. X. Yue, C. O. Yanez, S. Yao and K. D. Belfield, *Journal of the American Chemical Society*, 2013, **135**, 2112-2115.
21. J.-P. Malval, F. Morlet-Savary, X. Allonas, J.-P. Fouassier, S. Suzuki, S. Takahara and T. Yamaoka, *Chemical Physics Letters*, 2007, **443**, 323-327.
22. J.-P. Malval, S. Suzuki, F. Morlet-Savary, X. Allonas, J.-P. Fouassier, S. Takahara and T. Yamaoka, *Journal of Physical Chemistry A*, 2008, **112**, 3879-3885.
23. S. M. Kuebler, K. L. Braun, W. Zhou, J. K. Cammack, T. Yu, C. K. Ober, S. R. Marder and J. W. Perry, *Journal of*

RSC Advances Accepted Manuscript

Photochemistry and Photobiology a-Chemistry, 2003, **158**, 163-170.
24. W. Zhou, S. M. Kuebler, K. L. Braun, T. Yu, J. K. Cammack, C. K. Ober, J. W. Perry and S. R. Marder, *Science*, 2002, **296**, 1106-1109.
25. C. O. Yanez, C. D. Andrade and K. D. Belfield, *Chemical Communications*, 2009, 827-829.
26. R. Xia, J.-P. Malval, M. Jin, A. Spangenberg, D. Wan, H. Pu, T. Vergote, F. Morlet-Savary, H. Chaumeil, P. Baldeck, O. Poizat and O. Soppera, *Chemistry of Materials*, 2012, **24**, 237-244.
27. L. Steidl, S. J. Jhaveri, R. Ayothi, J. Sha, J. D. McMullen, S. Y. C. Ng, W. R. Zipfel, R. Zentel and C. K. Ober, *Journal of Materials Chemistry*, 2009, **19**, 505-513.
28. F. D. Saeva, E. Garcia and P. A. Martic, *Journal of Photochemistry and Photobiology a-Chemistry*, 1995, **86**, 149-154.
29. R. Xia, M. Jin, D. Wan, H. Pan and H. Pu, *Progress in Chemistry*, 2011, **23**, 1854-1861.
30. M. Jin, H. Hong, J. Xie, J.-P. Malval, A. Spangenberg, O. Soppera, D. Wan, H. Pu, D.-L. Versace, T. Leclerc, P. Baldeck, O. Poizat and S. Knopf, *Polymer Chemistry*, 2014, **5**, 4747-4755.
31. M. Jin, H. Xu, H. Hong, J.-P. Malval, Y. Zhang, A. Ren, D. Wan and H. Pu, *Chemical Communications*, 2013, **49**, 8480-8482.
32. S. Kawata, H.-B. Sun, T. Tanaka and K. Takada, *Nature*, 2001, **412**, 697-698.
33. G. S. He, L.-S. Tan, Q. Zheng and P. N. Prasad, *Chemical Reviews*, 2008, **108**, 1245-1330.
34. B. H. Cumpston, S. P. Ananthavel, S. Barlow, D. L. Dyer, J. E. Ehrlich, L. L. Erskine, A. A. Heikal, S. M. Kuebler, I. Y. S. Lee, D. McCord-Maughon, J. Q. Qin, H. Rockel, M. Rumi, X. L. Wu, S. R. Marder and J. W. Perry, *Nature*, 1999, **398**, 51-54.
35. H.-B. Sun and S. Kawata, *Two-Photon Photopolymerization and 3D Lithographic Microfabrication*, Berlin, Springer-Verlag edn., 2004.
36. B. H. Cumpston, S. P. Ananthavel, S. Barlow, D. L. Dyer, J. E. Ehrlich, L. L. Erskine, A. A. Heika, S. M. Kuebler, I.-Y. S. Lee, D. McCord-Maughon, J. Qin, H. Röckel, M. Rumi, X.-L. Wu, S. R. Marder and J. W. Perry, *Nature*, 1999, **398**, 51-54.
37. F. D. Saeva, D. T. Breslin and P. A. Martic, *Journal of the American Chemical Society*, 1989, **111**, 1328-1330.
38. W. Zhou, S. M. Kuebler, D. Carrig, J. W. Perry and S. R. Marder, *Journal of the American Chemical Society*, 2002, **124**, 1897-1901.
39. G. Pohlers, J. C. Scaiano and R. Sinta, *Chemistry of Materials*, 1997, **9**, 3222-3230.
40. M. Jin, J. Xie, J.-P. Malval, A. Spangenberg, O. Soppera, D.-L. Versace, T. Leclerc, H. Pan, D. Wan, H. Pu, P. Baldeck, O. Poizat and S. Knopf, *Journal of Materials Chemistry C*, 2014, **2**, 7201-7215.
41. P. Xiao, W. Hong, Y. Li, F. Dumur, B. Graff, J. P. Fouassier, D. Gigmes and J. Lalevee, *Polymer Chemistry*, 2014, **5**, 2293-2300.
42. S. Telitel, F. Ouhib, J.-P. Fouassier, C. Jerome, C. Detrembleur and J. Lalevee, *Macromolecular Chemistry and Physics*, 2014, **215**, 1514-1524.
43. M.-A. Tehfe, F. Dumur, P. Xiao, M. Delgove, B. Graff, J.-P. Fouassier, D. Gigmes and J. Lalevee, *Polymer Chemistry*, 2014, **5**, 382-390.
44. M.-A. Tehfe, F. Dumur, B. Graff, D. Gigmes, J.-P. Fouassier and J. Lalevee, *Macromolecular Chemistry and Physics*, 2013, **214**, 1052-1060.
45. M.-A. Tehfe, F. Dumur, B. Graff, J.-L. Clement, D. Gigmes, F. Morlet-Savary, J.-P. Fouassier and J. Lalevee, *Macromolecules*, 2013, **46**, 736-746.
46. J. Lalevée, M.-A. Tehfe, A. Zein-Fakih, B. Ball, S. Telitel, F. Morlet-Savary, B. Graff and J. P. Fouassier, *ACS Macro Letters*, 2012, **1**, 802-806.
47. T.-C. Lin, G. S. He, Q. Zheng and P. N. Prasad, *Journal of Materials Chemistry*, 2006, **16**, 2490-2498.
48. H. Wang, F. Jin, S. Chen, X.-Z. Dong, Y.-L. Zhang, W.-Q. Chen, Z.-S. Zhao and X.-M. Duan, *Journal of Applied Polymer Science*, 2013, **130**, 2947-2956.
49. X.-H. Qin, P. Gruber, M. Markovic, B. Plochberger, E. Klotzsch, J. Stampfl, A. Ovsianikov and R. Liska, *Polymer Chemistry*, 2014, **5**, 6523-6533.
50. Z. Li, J. Torgersen, A. Ajami, S. Muehleder, X. Qin, W. Husinsky, W. Holnthoner, A. Ovsianikov, J. Stampfl and R Liska, *Rsc Advances*, 2013, **3**, 15939-15946.
51. F. D. Saeva, D. T. Breslin and H. R. Luss, *Journal of the American Chemical Society*, 1991, **113**, 5333-5337.
52. F. D. Saeva and B. P. Morgan, *Journal of the American Chemical Society*, 1984, **106**, 4121-4125.
53. R. P. Subrayan, J. W. Kampf and P. G. Rasmussen, *Journal of Organic Chemistry*, 1994, **59**, 4341-4345.
54. P. Beak and T. A. Sullivan, *Journal of the American Chemical Society*, 1982, **104**, 4450-4457.
55. S. Erdur, G. Yilmaz, D. G. Colak, I. Cianga and Y. Yagci, *Macromolecules*, 2014, **47**, 7296-7302.
56. G. Yilmaz, B. Iskin, F. Yilmaz and Y. Yagci, *ACS Macro Letters*, 2012, **1**, 1212-1215.
57. S. Dadashi-Silab, H. Bildirir, R. Dawson, A. Thomas and Y. Yagci, *Macromolecules*, 2014, **47**, 4607-4614.
58. J. Liu, Z. Liu, L. Wang and H. Sun, *Chinese Science Bulletin*, 2014, **59**, 1097-1103.
59. J. Liu, Y. Qiao, Z. Liu and L. Wang, *Rsc Advances*, 2014, **4**, 21093-21100.
60. J. Yu, N. Xu, Q. Wei and L. Wang, *Journal of Materials Chemistry C*, 2013, **1**, 1160-1167.

RSC Advances Accepted Manuscript

This journal is © The Royal Society of Chemistry 20xx